Bioconjugate Chemistry

Article

pubs.acs.org/bc

Monoalkoxy BODIPYs—A Fluorophore Class for Bioimaging

Alexandra M. Courtis,[†] Sofia A. Santos,[†,∥,‡] Yinghua Guan,[§] J. Adam Hendricks,[†] Balaram Ghosh,[†,∥] D. Miklos Szantai-Kis,[†] Surya A. Reis,[∥] Jagesh V. Shah,[§] and Ralph Mazitschek*[,†,⊥]

[†]Center for Systems Biology and [∥]Center for Human Genetic Research, Massachusetts General Hospital, 185 Cambridge Street, Boston, Massachusetts 02114, United States

[‡]Instituto de Investigação do Medicamento (iMed.ULisboa), Faculdade de Farmácia, Universidade de Lisboa, Av. Professor Gama Pinto, 1640-003, Lisboa, Portugal

[§]Department of Systems Biology, Harvard Medical School, and Renal Division, Brigham and Women's Hospital, Boston, Massachusetts 02115, United States

[⊥]Broad Institute of Harvard and MIT, Cambridge, Massachusetts 02142, United States

Supporting Information

ABSTRACT: Small molecule fluorophores are indispensable tools for modern biomedical imaging techniques. In this report, we present the development of a new class of BODIPY dyes based on an alkoxy-fluoro-boron-dipyrromethene core. These novel fluorescent dyes, which we term MayaFluors, are characterized by good aqueous solubility and favorable *in vitro* physicochemical properties. MayaFluors are readily accessible in good yields in a one-pot, two-step approach starting from well-established BODIPY dyes, and allow for facile modification with functional groups of relevance to bioconjugate chemistry and bioorthogonal labeling. Biological profiling in living cells demonstrates excellent membrane permeability, low nonspecific binding, and lack of cytotoxicity.

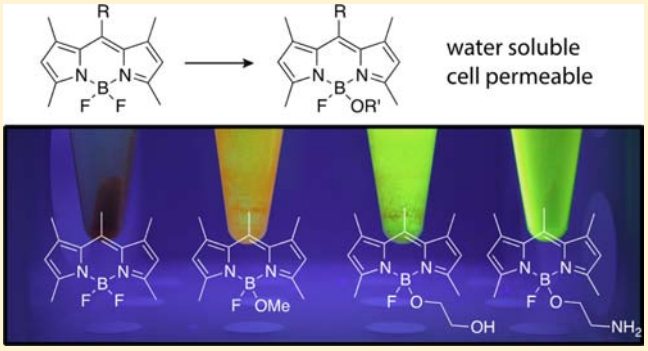

Tagging biologically active compounds of interest with a fluorescent tracer can allow for visualization of the spatial and temporal perturbation of biological systems in their endogenous state. Organic fluorophores are central for enabling imaging of dynamic biological systems at the single molecule to whole organism level.[1−5] For advanced optical microscopy techniques, small molecule dyes are orthogonal and often superior to alternatives, such as fluorescent proteins, due to their small size and ease of synthetic access. The identification of organic fluorophores suitable for labeling tool compounds of interest without perturbing biomolecular activity is an important but frequently problematic step in probe development. For live cell and *in vivo* imaging, an appropriate balance of aqueous solubility and lipophilicity is critical to ensure membrane permeability while minimizing nonspecific staining of lipid membranes.[6] Recent efforts to develop fluorescent dyes that satisfy the rigorous conditions required for routine live cell imaging have involved the development of nonplanar cyanine fluorophores, which exhibit low levels of nonspecific staining in preliminary cell studies.[7] Novel Near-IR probes have also been tested for routine live-cell imaging studies and point toward the importance of fluorophore development with explicit consideration of the eventual challenges to be faced in the imaging environment of interest.[8]

The ideal reporter group is a chemically stable, small fluorophore that readily trafficks through cellular compartments, maintains photostability in oxygenated aqueous media, and exhibits few drug-like attributes, which could interfere with a measurement of interest.[6] The fluorescent tag should have high quantitative brightness, photophysical properties that are independent of the local environment, good aqueous solubility (while remaining small and uncharged), and a favorable logP. Some of the most widely employed fluorophores for bioimaging are difluoro-boron-dipyrromethene dyes (BODIPYs) (**1**) (Figure 1).[9] BODIPY dyes fulfill most requirements for routine imaging and conjugation to small-molecule and protein targets of interest.

However, the traditional BODIPY core is inherently lipophilic and poorly water-soluble. These physical attributes drive partitioning of the fluorophore (or tagged small molecule) into lipophilic compartments, resulting in nonspecific staining of membranes and intracellular organelles. The typical background staining, which we attribute to the endoplasmic reticulum (ER) and Golgi membranes (see below), is commonly observed with cell permeable BODIPY dyes and other lipophilic dye classes (for examples, see refs 10−14). This characteristic can be troublesome as it significantly nonspecifi-

Received: December 19, 2013
Revised: May 2, 2014
Published: May 5, 2014

   dx.doi.org/10.1021/bc400575w | *Bioconjugate Chem.* 2014, 25, 1043−1051

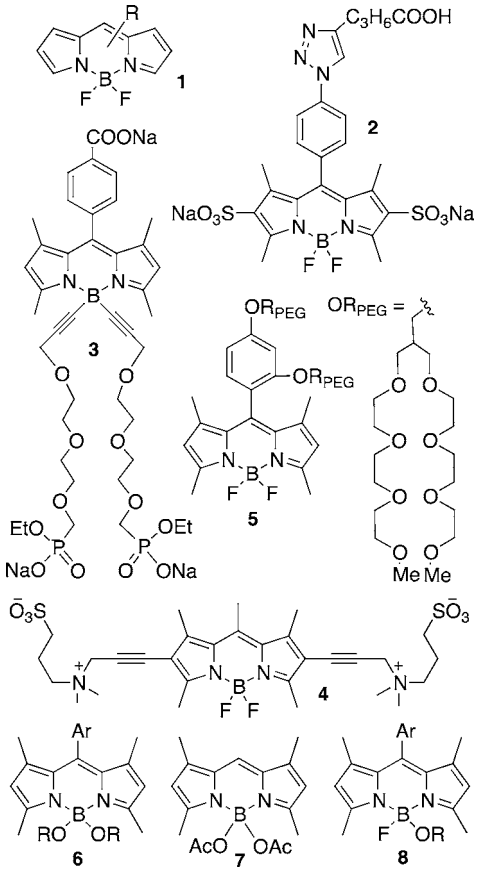

Figure 1. Structures of BODIPY dyes.

cally biases cellular distribution of labeled small molecules to membranes, which is often confused for specific target binding.

To counteract the main drawback of poor aqueous solubility, efforts to improve BODIPY dyes have strived to improve water solubility via the addition of charged functional groups such as sulfonates (**2**) and phosphonates (**3**), including the symmetric functionalization of the boron-core.[15] Ligands with a net formal charge of zero have also been explored such as zwitterionic sulfobetaines (**4**).[16] While all approaches yield BODIPY dyes with improved water solubility, the applicability of these derivatives for live cell and *in vivo* imaging is limited by the ionic character of the solubilizing groups, which impair membrane permeability, and often result in a significantly increased size of the fluorescent tag. Similarly, modification with multiple PEG-groups (**5**) can improve aqueous solubility, again at the cost of increased size (in some examples the solubilizing groups account for >80% of the total molecular weight).[17] Of interest in this context are dialkoxy (**6**) and diacetoxy (**7**) BODIPY dyes that have been reported to exhibit improved aqueous solubility compared to the difluoro analogues.[18−20] However, no reports studying the application of such probes in biological systems have been published.

In this work, the aim was to develop a method to improve the biological imaging compatibility of the BODIPY fluorophore while ideally retaining opportunities for multimodal imaging and bioconjugate chemistries. The presented approach originates from our group's recent development of BODIPYs for hybrid optical/positron emission tomography imaging.[21] Instead of $^{19}F/^{18}F$ exchange, we explore selective access to singly alkoxy-substituted (core monoalkoxy) BODIPY (CMA-BODIPY) dyes and evaluate the applicability of these derivatives for biological imaging in comparison to BODIPY and dialkoxy-BODIPY dyes.

We found that retaining one fluorine on the dye scaffold allows for exquisite tuning of the physiochemical properties of the fluorophore while providing an attachment site for bioconjugate and multimodal imaging chemistries. Most importantly, CMA-BODIPYs are characterized by excellent membrane permeability, homogeneous distribution, and low nonspecific background in living cells. Prior to our work, following published procedures, CMA-BODIPYs (**8**) were only obtained as byproducts in mixtures with the corresponding dialkoxy derivatives (**6**) that are difficult to separate.[18,20] Herein, we report efficient methodology to selectively access singly alkoxy-substituted BODIPYs and evaluate their applicability for live cell imaging in comparison to BODIPY and dialkoxy-BODIPY dyes.

RESULTS

Synthetic Approach. *Methodology.* We selected BODIPY (**9**) as a model substrate since it is well established and provides direct access to dimethoxy BODIPY (**10**) as a reference compound (Figure 2a).[18,20,22] To selectively substitute only one fluorine, we applied a two-step one-pot strategy, inspired by our previous work on $^{19}F/^{18}F$ exchange on BODIPYs for hybrid optical/positron emission tomography imaging.[21] The synthesis relies on abstraction of a single fluoride from the BF_2-core to generate a borenium intermediate (**11**).[25,26] We found this intermediate readily reacts with suitable alcohols to yield

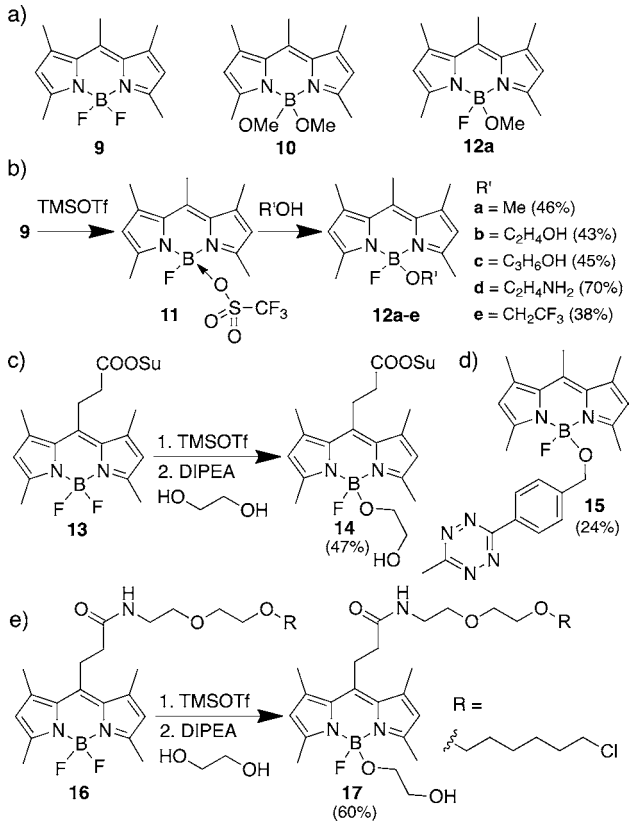

Figure 2. (a) Structures of BODIPY analogues **9**, **10**, and **12a**. (b) One-pot synthesis of MayaFluor analogues **12a−e**. Isolated yield after purification is given in parentheses. (c) Synthesis of MayaFluor **14** and (d) tetrazine-functionalized MayaFluor **15**. HaloTag-ligand conjugated BODIPY **16** and MayaFluor **17**.

dx.doi.org/10.1021/bc400575w | *Bioconjugate Chem.* 2014, 25, 1043−1051

the desired monoalkoxy-BODIPY (**12**) in high yields without the formation of dialkoxy BODIPY (Figure 2b).

Specifically, CMA-BODIPYs were accessed by activation of difluoro-BODIPY with excess trimethylsilyl trifluoromethanesulfonate (TMSOTf) to yield the BODIPY-OTf (**11**) intermediate,[26] followed by addition of a suitable alcohol to afford the desired monoalkoxy-BODIPY in moderate to good yields (**12a**–**e**). The activated BODIPY-OTf (**11**) is not stable for a prolonged time under the reaction conditions and slowly degrades, forming the free pyrrole ligand. Therefore, the addition of the desired alcohol ligand has to be timed carefully. Simultaneous addition of DIPEA as a mild, non-nucleophilic base to buffer the acidity of the crude reaction solution was found to be beneficial.

This synthesis is highly modular and allows for easy access to an array of different alkoxy BODIPY derivatives. Notably, the presented methodology is compatible with primary alcohol, primary amine, NHS-ester, and tetrazine functional groups. We therefore predict that this strategy will tolerate a wider number of functionalities. For example, as illustrated in Figure 2c, the NHS-functionalized BODIPY **13** was efficiently converted into the glycol-analogue **14**. We expect that these functionalities would be synthetically incompatible with the existing strategies (referenced above) to access these analogues as mono and dialkoxy mixtures of compounds such as **12b**.

Of particular interest is the direct functionalization with tetrazines as illustrated by BODIPY **15** (Figure 2d), which was isolated in 24% yield. Tetrazines have recently received much appreciation for their applications in bio-orthogonal catalyst-free "click-reactions" with *trans*-cyclooctenes or cyclopropenes, respectively.[27−29] A unique feature of tetrazines is their ability to quench green to red emitting fluorescent dyes by a FRET based mechanism.[29] Reaction of **15** with *trans*-cyclooctene (TCO) in PBS results in greater than 30-fold fluorescence increase (SI Figure 1 and Video 1). Probes like **15** will therefore be useful tools to visualize TCO or cyclopropene-labeled biological targets in live cells.

Physicochemical Characterization of CMA-BODIPYs. To assess the suitability of CMA-BODIPY dyes for biological applications, we investigated their physical properties in direct comparison to relevant reference compounds, difluoro **9** and dimethoxy **10** BODIPY in aqueous buffer at physiological pH.

Solubility. We first investigated the solubility characteristics in aqueous buffer at physiological pH. Dry powders of the respective compounds in excess were used to prepare saturated solutions in PBS (pH = 7.4). The alkoxy derivatives have excellent water solubility, while the difluoro-BODIPY **9** appears to be virtually insoluble in PBS. Quantitative measurements showed that the alkoxy derivatives are generally soluble at medium to high micromolar concentrations in PBS without the requirement of co-solvents or detergents (Table 1).

Lipophilicity. Next, we determined the $logD_{7.4}$, which is an important characteristic to gauge membrane permeability and the propensity of a small molecule to distribute between aqueous and hydrophobic cellular compartments. Compounds with a logD of 1−3 strike this balance best and demonstrate the greatest membrane permeability.[6] The increased aqueous solubility of CMA-BODIPYs correlates with a lower $logD_{7.4}$ compared to difluoro BODIPY **9** (Table 1). Notably, the methoxy (**12a**) and glycol analogues (**12b**,**c**) exhibit ideal logDs of 1.4 and 2.2, respectively. The CMA-BODIPY **12d**, as a result of the protonated amine group, is slightly more hydrophilic (logD = 0.32). In contrast, the difluoro-BODIPY **9** had an unfavorable logD of >5.

Table 1. Physicochemical Characterization of BODIPYs

	LogD[a]	solubility [μM][b]	Φ_{fl}[c]	λ_{max}abs[d] [nm]	λ_{max}em[d] [nm]	ε[e] [M^{-1} cm^{-1}]
9	>5	3	n/a	457[f]	513[h]	10 300[f]
				494[g]		86 500[g]
10	2.4	n/a	0.35	491	506[f]	71 300[f]
12a	1.4	24	0.33	492[f]	520[f]	70 900
12b	2.2	122	0.47	491[f]	504[f]	66 300[f]
				495[g]		77 200[g]
12c	2.2	48	0.35	491[f]	504[f]	66 700[f]
12d	0.32	450	n/a	492[f]	n/a	50 600[f]
12e	>5	3	n/a	491[f]	510[f]	54 800[f]
				495[g]	513[h]	79 600[g]
16	>5	2.4	n/a	n/a	n/a	n/a
17	3.85	230	n/a	n/a	n/a	n/a

[a]LogD was determined via the shake-flask method by partitioning a saturated solution of the probes in phosphate buffered saline (PBS) (pH = 7.4) with 1-octanol. [b]Solubility was determined in PBS (pH = 7.4) from the concentration of a saturated solution of each probe. [c]Quantum yields were determined in ddH_2O using Fluorescein in 0.1 M NaOH as a reference. [d]Spectral properties were determined in ddH_2O unless otherwise indicated. [e]Molar extinction coefficient was determined according to the Beer−Lambert law in triplicate using a quartz cuvette. [f]H_2O. [g]MeOH. [h]DMSO. Absorbance and emission spectra are provided as Supporting Information. For absorbance and emission spectra see SI Figure 4.

Aqueous Stability. To further probe the persistence of the chemical integrity of the dyes and identify fluorescent degradation products that would not result in reduction of overall fluorescence (Figure 3) we also monitored the stability

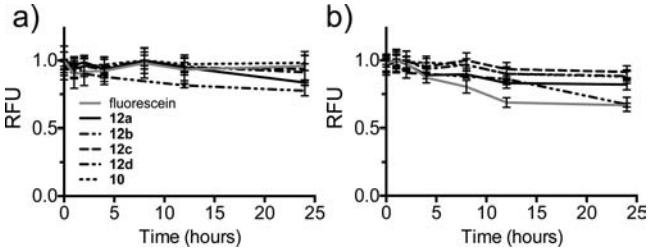

Figure 3. Time-dependent stability of **10**, **12a**−**d** at 1 μM and room temperature in (a) PBS (pH = 7.4) and (b) RPMI 1640 Media; (−) phenol-red; (+) 10% fetal bovine serum (FBS).

of representative BODIPY derivatives over 24 h in PBS by LC-MS. The stability data obtained at room temperature and 37 °C (SI Figures 2 and 3) demonstrate that the monoalkoxy analogues exhibit good to very good stability. In contrast, the dimethoxy reference compound **10** was characterized by increased hydrolysis and underwent near-quantitative degradation after 24 h incubation at 37 °C. This data stands in sharp relief to the monomethoxy derivative **12a** that experienced only modest degradation under these conditions. Importantly, monoalkoxy derivatives with incrementally larger substituents were characterized by improved stability displaying only minor or no hydrolysis. Detailed LC-MS analysis revealed that both difluoro **9** and fluoro-alkoxy **12** BODIPY hydrolyze to form the common 4-fluoro-4-hydroxy BODIPY as the primary degradation product, while the formation of 4-methoxy-4-hydroxy BODIPY was observed for compound **10**.

dx.doi.org/10.1021/bc400575w | *Bioconjugate Chem.* 2014, 25, 1043−1051

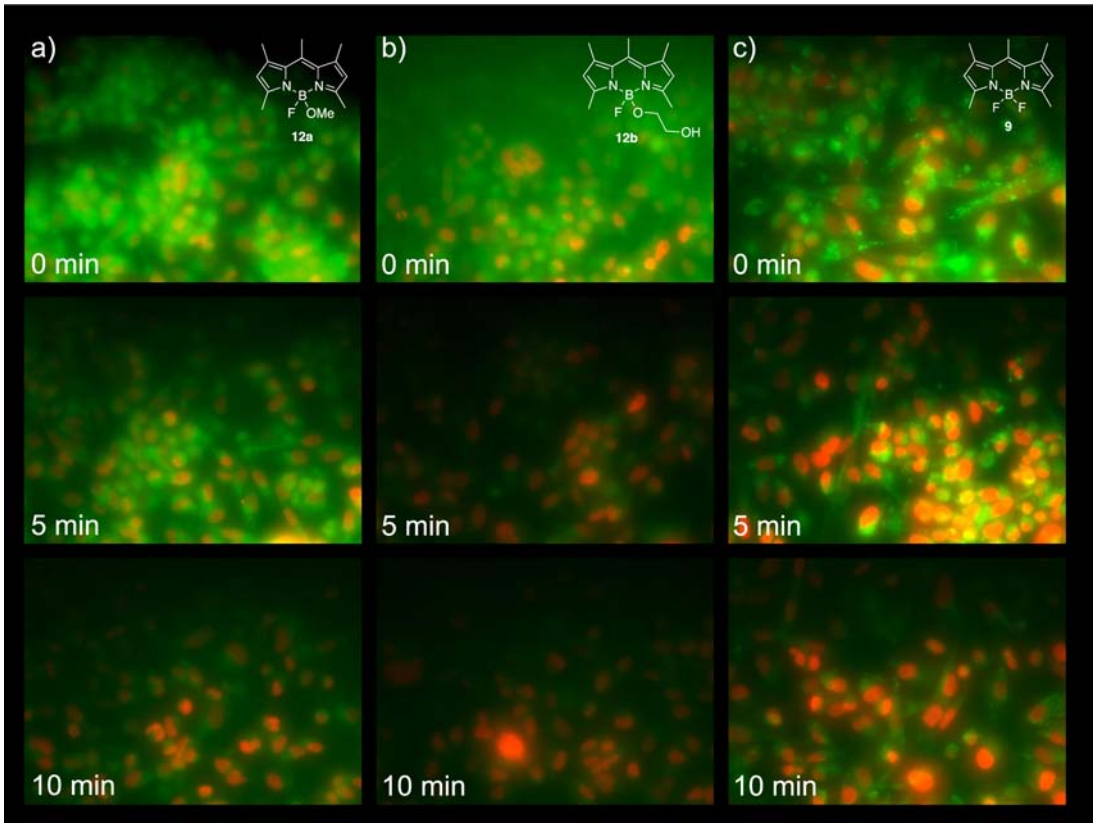

Figure 4. Cellular uptake and intracellular distribution and wash-out kinetics of MayaFluors **12a** and **12b** in comparison to difluoro BODIPY **9**. MD-MBA 231 cells (expressing mCherry labeled histone H2B) were treated for 30 min at 10 μM followed by media replacement every 5 min to remove excess dye. Both CMA-BODIPYs show relatively homogeneous even intracellular distribution compared to BODIPY **9**, which seems to primarily locate to endosomal structures. **12a** and **12b** are efficiently washed out within 10 min in contrast to **9**, which is retained. Each image was acquired from an independent replicate well, to ensure no confounding photobleaching effects. (High resolution images are provided in SI Figure 5.) All images were acquired with identical microscopy settings and have not been processed differently to allow for direct comparison. All images are to scale.

Optical Properties. The absorbance and emission spectra of CMA-BODIPYs **12a−e** measured in aqueous solution were virtually identical to the corresponding absorbance/emission profile of **9**, which was measured in DMSO because of limited aqueous solubility (Table 1 and SI Figure 4). The quantum yield (QY) and therefore the brightness of fluorescent dyes can be strongly dependent on the polarity of the environment, and some dye classes have been shown to be poorly fluorescent in aqueous media.[30] Due to poor overall aqueous solubility, reference data for BODIPY dyes is generally limited to solvents such as methanol or halogenated hydrocarbons. However, the QY in aqueous environments is a more relevant metric for biological applications. We therefore determined QYs of CMA-BODIPYs in water (Table 1). All tested compounds that were sufficiently soluble exhibited good quantum yields of 0.3−0.5, which is comparable to the results reported under the same conditions for BODIPY dyes containing the aforementioned solubilizing sulfobetaines **4** and the widely used cyanine dyes.[17] The QY of difluoro-BODIPY **9** is nearly quantitative in MeOH; however, fluorescence is almost completely suppressed in water, possibly as a result of self-quenching due to aggregation.

In addition to solvent polarity, pH can also impact the spectral properties of organic fluorophores like fluorescein and hydroxycoumarin. While this characteristic can be exploited for the development of pH-sensors, it is not a desirable photophysical characteristic for fluorescent labeling and tracking small molecules or proteins.[1] As CMA-BODIPYs do not feature functional groups that are ionizable under physiologically relevant pH values, the fluorescence intensity is expected to be pH independent as observed with regular BODIPYs.[31] Using CMA-BODIPY **12a** as representative example, we did not observe a significant change in fluorescence intensity over a broad pH range (pH = 3−10) (see SI Figure 5).

To demonstrate that the favorable properties of CMA-BODIPYs are retained upon conjugation to small molecules, we synthesized HaloTag functionalized BODIPY **16** and CMA-BODIPY **17** from the common NHS-ester precursor **13** (Figure 2e). HaloTag ligands bind selectively and covalently to HaloTag, a small protein that can be expressed as a fusion protein with a target protein of interest, to allow for selective labeling of intracellular targets.[32] We selected the HaloTag system over other tags like SNAP-tag and CLIP-tag as it would represent a demanding test system; the chloroalkane HaloTag ligand is very hydrophobic. The solubility of compound **17** in PBS was 231 μM, almost 2 orders of magnitude greater than the BODIPY **16** (Table 1). Similarly, this increased aqueous solubility also translated into an improved logD.

***In Vitro* Profiling.** *Live Cell Imaging.* To evaluate the applicability of CMA-BODIPYs for live cell imaging, we interrogated representative derivatives for their ability to penetrate mammalian cell membranes and their propensity for nonspecific background staining. MD-MBA-231 cells expressing mCherry-histone H2B were incubated with 10 μM

dx.doi.org/10.1021/bc400575w | *Bioconjugate Chem.* 2014, 25, 1043−1051

of **12a**, **12b**, and **9**, respectively. Following a 30 min incubation at 37 °C, the culture medium was replaced every 5 min to remove excess dye. Live cells were imaged by multichannel fluorescence microscopy to assess penetration efficiency and subcellular staining patterns and estimate wash-out kinetics (Figure 4, SI Figures 6, 7). All tested compounds exhibited efficient cell uptake. However, cellular uptake kinetics significantly differ for CMA-BODIPYs **12a−c** compared to BODIPY **9**. Quantitative intracellular studies demonstrated that even at short incubation periods (5 min) and low concentrations (100 nM) **12a−c** rapidly enter cells to a high degree and washed out efficiently, which is consistent with the favorable logD of these compounds. In contrast, the highly lipophilic parent compound, BODIPY **9**, showed minimal cellular uptake after short incubation (SI Figure 8).

Importantly, BODIPY **9** displayed a subcellular perinuclear reticulate staining pattern that is consistent with nonspecific binding to the ER and Golgi, reminiscent of other reports employing hydrophobic BODIPY dyes for live-cell imaging (Figure 4c).[10−14] We have validated this experimentally via costaining experiments with BODIPY **9** and ER-Tracker Red, demonstrating a high degree of colocalization (SI Figure 9). In contrast, CMA-BODIPYs showed little to no nonspecific staining and are distributed throughout the cells (Figure 4a,b). Both CMA-BODIPYs are efficiently washed out by replacement of dye-free media, in sharp contrast to compound **9**, which is retained. Similar results were obtained after longer wash cycles.

To assess potential cytotoxic effects of CMA-BODIPYs, we incubated MCF-7 cells with 10 μM **9**, **12a**, and **12b**, respectively. Cell viability was determined using CellTiter-Glo. Even after prolonged incubation for 48 h none of the tested dyes reduced cell viability (SI Figure 10). Having established the favorable membrane permeability and low nonspecific background staining of CMA-BODIPYs, we expect that these and related MayaFluors will have far reaching applications for rapid and specific imaging of elusive biological targets in living cells.

DISCUSSION

The BODIPY dyes are an exciting fluorophore class for diverse imaging applications. They are particularly promising for tagging bioactive compounds for intracellular live cell imaging. However, poor aqueous solubility and high lipophilicity significantly limit the scope of BODIPYs for chemogenomic studies. Although extensive efforts have focused on developing derivatives that have improved water solubility by either installing charged substituents or large PEG chains, these modifications also severely impair or abolish cell permeability.

In this work we report the development of methodology to selectively substitute one of the two canonical fluorides common to most BODIPY dyes with alkoxy ligands, and show that the resulting dyes are highly soluble and cell permeable.

This new class of BODIPY fluorophores, which we term MayaFluors, has significantly improved physicochemical properties that are ideally suited for biological applications. MayaFluors retain the optical attributes of the parent BODIPY dye class while enjoying significant improvements in their lipophilicity. Importantly, we demonstrate the robust optical and chemical stability of these probes under cell culture imaging conditions. We have validated the applicability of these dyes as fluorescent reporters for live cell imaging and demonstrate that MayaFluors have excellent membrane permeability and show little to no nonspecific staining. Furthermore, we did not observe a differential propensity of MayaFluors to photobleach compared to conventional difluoro BODIPY derivatives. Additionally, MayaFluors did not impact the viability of living cells, even after prolonged incubation at concentrations much higher than would be required for imaging applications.

We hypothesize that the low propensity of MayaFluors to insert into biological membranes is the result of aqueous solubility imparted by the increased out of plane dipole moment these analogues experience as opposed to difluoro BODIPYs. Furthermore, addition of the alkoxy substituent disrupts the planarity of the BODIPY core, which is expected to reduce their ability to self-aggregate and insert into lipid leaflets via the formation of $\pi-\pi$ stacks.[33] One interesting feature of MayaFluors for future study is the tetrahedral coordination environment of the boron core and the potential to access chiral MayaFluors from the corresponding asymmetrically substituted homochiral BODIPY precursor. These derivatives would represent interesting materials for nonlinear imaging of chiral environments and second harmonic generation imaging at interfaces.[34]

Our synthetic methodology is the first approach to selectively access MayaFluors and is compatible with a broad array of functional groups commonly utilized in chemogenomic approaches. The method allows for direct modification of the well-established BODIPY dyes and provides easy access to diversely functionalized reporters. Importantly, the alkoxy substituent presents an additional and unique attachment site, which can be readily deployed as modular tether for multiple conjugation chemistries without perturbing the fluorophore scaffold. Notably, we foresee applicability for the installment of click-tags and isotope bearing ligands for dual modality imaging (e.g., PET and MRI).[21,35] The broad impact of our approach is demonstrated herein by reaction of ^{13}C-methanol with BODIPY **11** to yield ^{13}C-labeled **12a** ([**13C**]-**12a**), a direct MRI probe and surrogate compound for ^{11}C-PET imaging. Alternatively, small molecules of interest that feature an appropriate hydroxyl group may be directly functionalized by reaction with the BODIPY-OTf intermediate.

EXPERIMENTAL PROCEDURES

Chemicals and Reagents. Reagents were purchased from Chem-Impex International, Aldrich, Fluka, and Sigma-Aldrich Co. and used without further purification unless otherwise noted. All solvents for syntheses were anhydrous. Thin layer chromatography was performed with precoated aluminum-backed TLC plates obtained from VWR: Aluminum Oxide 60, Neutral F254 & Silica Gel 60, Neutral F254. Visualization of TLC plates was performed with ninhydrin, iodine, or an UVGL-25 Compact UV Lamp 254/365 UV (UVP 115 V ~ 60 Hz/0.16 Amps). Purifications were performed either with aluminum oxide (Brockmann I, Sigma-Aldrich), silica (Silicycle, Quebec City, Canada), or on a Biotage Isolera 4 Purification System equipped with a 200−400 nm diode array detector. For flash purifications, Biotage SNAP Flash Chromatography Cartridges were used (KP-C18-Sil & KP-NH).

Instrumentation. Analytical LC-MS was performed on a Waters 2545 HPLC equipped with a 2998 diode array detector, a Waters 3100 ESI-MS module, using a XTerraMS C18 5 μm, 4.6 × 50 mm column at a flow rate of 5 mL/min with a linear gradient (95% A: 5% B to 100% B with 90 and 30 s hold at

dx.doi.org/10.1021/bc400575w | Bioconjugate Chem. 2014, 25, 1043−1051

100% B, solvent A = water + 0.1% formic acid, solvent B = acetonitrile + 0.1% formic acid). Proton and carbon nuclear magnetic resonance (^{1}H and ^{13}C NMR spectra) were recorded on a Varian AS-400 (400 MHz) spectrometer. Chemical shifts for protons are reported in parts per million (ppm) and are referenced to residual solvent peaks for C_6H_6 (7.16 ppm), $CHCl_3$ (7.26 ppm), and CH_3CN (1.94 ppm). Data is reported as follows: chemical shift, integration, multiplicity (s = singlet, d = doublet, t = triplet, m = multiplet), and coupling constants (Hz). High-resolution mass-spectra were performed on a Bruker Daltonics APEXIV 4.7 T Fourier transform ion cyclotron resonance mass spectrometer (FT-ICR-MS), with ESI (Electro Spray Ion) source. Instant JChem was used for structure database management, search and prediction (Instant JChem 5.9.3, 2012, ChemAxon (http://www.chemaxon.com)).

Synthetic Procedures. 1,3,5,7,8-Pentamethyl BODIPY (**9**) (4,4-Difluoro-1,3,5,7,8-pentamethyl-4-bora-*3a,4a*-diaza-*s*-indacene), 1,3,5,7-tetramethyl BODIPY-NHS (**13**) (4,4-difluoro-1,3,5,7-tetramethyl-8-(*N*-succinimidyl carboxypropyl)-4-bora-*3a,4a*-diaza-*s*-indacene) and (4-(6-methyl-1,2,4,5-terazin-3-yl)-phenyl)methanol were synthesized according to literature procedures.[22−24]

1,3,5,7,8-Pentamethyl dimethoxy BODIPY (**10**) (4,4-Dimethoxy-1,3,5,7,8-pentamethyl-4-bora-*3a,4a*-diaza-*s*-indacene) was synthesized following the procedure published by Tahtaoui et al. for aryl-analogues.[20] ^{1}H NMR (400 MHz, benzene-d_6) δ 5.84 (s, 2H), 3.16 (s, 6H), 2.69 (s, 6H), 2.07 (s, 6H), 1.99 (s, 3H).^{13}C NMR (101 MHz, benzene-d_6) δ 154.26, 141.09, 139.02, 133.97, 121.27, 49.25, 17.41, 16.22, 14.82.

General Procedure A. In a round-bottom flask, 1,3,5,7,8-Pentamethyl BODIPY **9** (1 equiv) was dissolved in CH_2Cl_2 for a final concentration of 1.9 mM. The solution was chilled at 0 °C on an ice−water bath and, under stirring, TMSOTf (5 equiv) was added from a 10% (v/v) stock solution in $CHCl_3$. The reaction was allowed to proceed for 2 min and 30 s. Then, a premixed solution of alcohol (∼100 equiv) and DIPEA (10 equiv) was rapidly injected into the reaction. The mixture was then partitioned between 1:1 CH_2Cl_2:H_2O. The organics were washed 3X with H_2O + 10% NaCl (sat), dried over Na_2SO_4, gravity filtered, and solvents removed *in vacuo* at room temperature. All purifications were performed immediately after obtaining the dry, crude product.

1,3,5,7,8-Pentamethyl fluoro methoxy BODIPY ***12a*** *(4-fluoro-4-methoxy-1,3,5,7,8-pentamethyl-4-bora-3a,4a-diaza-s-indacene).* Purified on aluminum oxide column (5:1 Toluene:MeCN → 1:1 Toluene:MeCN) yielding an orange powder (14 mg, 0.051 mmol, 46%). HRMS: $C_{15}H_{20}BFN_2O$ $[M + Na]^+$ Calculated: 297.1558, Found: 297.1550/ $[M-F]^+$ Calculated: 255.1676, Found: 255.1665. ^{1}H NMR (400 MHz, benzene-d_6) δ 5.76 (s, 2H), 3.11 (s, 3H), 2.66 (s, 6H), 1.99 (s, 6H), 1.87 (s, 3H). ^{13}C NMR (101 MHz, benzene-d_6) δ 154.08, 141.42, 139.75, 133.17, 121.25, 49.12 (d, J = 6.9 Hz), 17.22, 16.07, 14.75 (d, J = 2.6 Hz).

1,3,5,7,8-Pentamethyl fluoro methoxy(13C) BODIPY ***[13C]-12a*** *(4-fluoro-4-methoxy-1,3,5,7,8-pentamethyl-4-bora-3a,4a-diaza-s-indacene).* Purified on aluminum oxide column (5:1 Toluene:MeCN → 1:1 Toluene:MeCN) yielding an orange powder (7 mg, 0.025 mmol, 64%). HRMS: $C_{14}(13C)H_{20}BFN_2O$ $[M-F]^+$ Calculated: 256.1675, Found: 256.1686 [**13C**]-**12a** ^{1}H NMR (400 MHz, benzene-d_6) δ 5.76 (s, 2H), 3.11 (d, J = 138.2 Hz, 3H), 2.66 (d, J = 1.2 Hz, 6H), 2.00 (s, 6H), 1.88 (s, 3H). ^{13}C NMR (101 MHz, benzene-d_6) δ 154.09, 141.39, 139.71, 133.17, 121.25, 49.13 (d, J = 6.9 Hz), 17.22, 16.07, 14.76 (d, J = 2.6 Hz).

1,3,5,7,8-Pentamethyl fluoro glycol BODIPY ***12b*** *(4-fluoro-4-hydroxyethoxy-1,3,5,7,8-pentamethyl-4-bora-3a,4a-diaza-s-indacene).* Purified on aluminum-oxide column (1:1 Toluene:MeCN → 1:5 Toluene:MeCN +1% MeOH) yielding an orange powder (20 mg, 0.066 mmol, 43%). HRMS: $C_{16}H_{22}BFN_2O_2$ $[M + Na]^+$ Calculated: 327.1664, Found: 327.1673. ^{1}H NMR (400 MHz, benzene-d_6) δ 5.74 (s, 2H), 3.56 (q, J = 5.3 Hz, 2H), 3.10 (t, J = 4.9 Hz, 2H), 2.60 (s, 6H), 2.21 (t, J = 6.2 Hz, 1H), 1.98 (s, 6H), 1.86 (s, 3H). ^{13}C NMR (101 MHz, benzene-d_6) δ 154.34, 141.76, 140.26, 133.32, 121.72, 63.93, 63.39 (d, J = 5.7 Hz), 17.52, 16.39, 15.12 (d, J = 2.8 Hz).

1,3,5,7,8-Pentamethyl fluoro hydroxypropoxy BODIPY ***12c*** *(4-fluoro-4-hydroxypropoxy-1,3,5,7,8-pentamethyl-4-bora-3a,4a-diaza-s-indacene).* Purified on aluminum oxide column (5:1 Toluene:MeCN → 1:5 Toluene:MeCN + 1% MeOH) yielding an orange powder (22 mg, 0.069 mmol, 45%). HRMS: $C_{17}H_{24}BFN_2O_2$ $[M+Na]^+$ Calculated: 341.1821, Found: 341.1813. ^{1}H NMR (400 MHz, benzene-d_6) δ 5.74 (s, 2H), 3.80 (dd, J = 10.4, 5.2, 2H), 3.36 (t, J = 5.3, 1H), 3.21 (t, J = 5.6, 2H), 2.63 (s, 6H), 1.98 (s, 6H), 1.86 (s, 3H), 1.61−1.55 (m, 2H). ^{13}C NMR (101 MHz, benzene-d_6) δ 154.11, 141.39, 139.92, 133.05, 121.41, 63.37, 61.94 (d, J = 5.6 Hz), 33.95, 17.18, 16.06, 14.78 (d, J = 3.0 Hz).

1,3,5,7,8-Pentamethyl fluoro aminoglycol BODIPY ***12d*** *(4-fluoro-4-aminoethoxy-1,3,5,7,8-pentamethyl-4-bora-3a,4a-diaza-s-indacene).* Purified on a KP-NH Biotage cartridge (9:1 Toluene:MeCN → 1:3 Toluene:MeCN) yielding an orange powder (32 mg, 0.106 mmol, 70%). HRMS: $C_{16}H_{23}BFN_3O$ $[M-F]^+$ Calculated: 284.1942, Found: 284.1946. ^{1}H NMR (400 MHz, benzene-d_6) 5.76 (s, 2H), 3.07 (t, J = 5.3 Hz, 2H), 2.80−2.61 (m, 8H), 2.00 (s, 6H), 1.88 (s, 3H), 1.15 (s, 2H).

1,3,5,7,8-Pentamethyl fluoro trifluoroethoxy BODIPY ***12e*** *(4-fluoro-4-trifluoroethoxy-1,3,5,7,8-pentamethyl-4-bora-3a,4a-diaza-s-indacene).* Purified on a C18 Biotage cartridge (95:5 H_2O:MeCN → 5:95 H_2O:MeCN) yielding an orange powder (15 mg, 0.044 mmol, 38%). HRMS: $C_{16}H_{19}BF_4N_2O$ $[M + Na]^+$ Calculated: 365.1432, Found: 365.1429. ^{1}H NMR (400 MHz, $CDCl_3$) 6.07 (s, 2H), 3.25 (q, J = 9.3 Hz, 2H), 2.59 (s, 3H), 2.52 (s, 6H), 2.42 (s, 6H). ^{13}C NMR (101 MHz, $CDCl_3$) 154.34, 141.35, 140.94, 132.68, 128.29−127.55 (m), 121.73, 60.97 (qd, J = 34.5, 7.4 Hz), 17.57, 16.58, 14.48 (d, J = 2.8 Hz).

(4-Fluoro-4-hydroxyethoxy-1,3,5,7-tetramethyl-8-(N-succinimidyl carboxypropyl)-4-bora-3a,4a-diaza-s-indacene) ***14.*** To BODIPY-NHS **13** (20 mg, 0.048 mmol) in $CHCl_3$ (10 mL) was added TMSOTf from a 10% (v/v) stock solution in $CHCl_3$ (434 μL, 0.24 mmol) under stirring at 0 °C. After 4 min activation, the reaction was rapidly quenched with a premixed solution of ethylene glycol (1.38 μL, 2.4 mmol) and DIPEA (52 μL, 0.30 mmol). After 5 min, the reaction was poured into 100 mL of 1:1 2-methyltetrahydrofuran:NaCl (sat). The organic layer was dried over $MgSO_4$, filtered, and the solvents removed *in vacuo*. Purified on a silica gel column (1:1 Toluene:MeCN → 1:10 Toluene:MeCN) yielding an orange solid (10.4 mg, 0.023 mmol, 47%). HRMS: $C_{22}H_{27}BFN_3O_6$ $[M + Na]^+$ Calculated: 482.1884, Found: 482.1890. ^{1}H NMR (400 MHz, $CDCl_3$) δ 6.08 (s, 2H), 3.53 (q, J = 5.1 Hz, 2H), 3.45−3.40 (m, 2H), 2.96 (t, J = 4.8 Hz, 2H), 2.92−2.84 (m, 6H), 2.52 (s, 6H), 2.45 (s, 6H).

1,3,5,7,8-Pentamethyl fluoro benzyltetrazine BODIPY ***15*** *(4-fluoro-4-(4-(6-methyl-1,2,4,5-tetrazin-3-yl)phenyl)-methoxy-1,3,5,7,8-pentamethyl-4-bora-3a,4a-diaza-s-indacene).* To 1,3,5,7,8-pentamethyl BODIPY **9** (5.4 mg, 0.021 mmol) in 4 mL $CHCl_3$ was added TMSOTf from a 10% (v/v) stock solution in $CHCl_3$ (110 μL, 0.062 mmol) under stirring at 0 °C. After 3 min activation, the reaction was rapidly quenched with (4-(6-methyl-1,2,4,5-terazin-3-yl)phenyl)-methanol (25.0 mg, 0.124 mmol) and DIPEA (22 μL, 0.12 mmol) in 4 mL $CHCl_3$. The reaction mixture was allowed to warm to room temperature over 15 min and then 20 mL 1:1 CH_2Cl_2:H_2O was added. Subsequently, the organic layer was washed 3X with H_2O + 10% NaCl (sat). The organic layer was dried over Na_2SO_4, gravity filtered, and solvents were removed *in vacuo* at room temperature. Purified on an aluminum oxide column (10:1 Toluene:MeCN → 1:1 Toluene:MeCN) yielding a red-orange powder (2.2 mg, 0.005 mmol, 24%). HRMS: $C_{24}H_{26}BFN_6O$ $[M + Na]^+$ Calculated: 467.2152, Found: 467.2150. ^{1}H NMR (400 MHz, benzene-d_6) δ 8.62 (d, J = 8.3 Hz, 2H), 7.44 (d, J = 8.5 Hz, 2H), 5.69 (s, 2H), 4.29 (s, 2H), 2.59 (s, 6H), 2.42 (s, 3H), 1.97 (s, 6H), 1.88 (s, 3H).

(4,4-Difluoro-1,3,5,7-tetramethyl-8-(3-((2-(2-((6-chlorohexyl)oxy)ethoxy)ethyl)amino)-3-oxopropyl)-4-bora-3a,4a-diaza-s-indacene) ***16.*** BODIPY-NHS **13** (12.5 mg, 0.030 mmol) was dissolved in CH_2Cl_2 (2 mL). To this solution was added 2-(2-((6-chlorohexyl)oxy)ethoxy)ethanamine hydrochloride (6.7 mg, 0.03 mmol) and DIPEA (16 uL, 0.09 mmol) under stirring at room temperature. After 30 min, the solvent was removed *in vacuo* at room temperature. Purified on a silica gel column (100% Toluene →1:1 Toluene:MeCN) yielding an orange solid (5.8 mg, 0.011 mmol, 37%). MS: $C_{26}H_{39}BClF_2N_3O_3$. Exact mass: 525.27; ES-$[M-H]^-$ Found: 524.24; ES+$[M + Na]^+$ Found: 548.31. ^{1}H NMR (400 MHz, benzene-d_6) δ 5.67 (s, 2H), 5.41 (brs, 1H-NH), 3.32−3.30 (m, 6H), 3.21−3.07 (m, 8H), 2.60 (s, 6H), 2.15 (s, 6H), 1.82−1.78 (m, 2H), 1.42−1.36 (m, 4H), 1.16−1.06 (m, 4H). ^{13}C NMR (101 MHz, benzene-d_6) δ 170.40, 154.44, 144.47, 140.49, 131.30, 121.82, 71.29, 70.34, 70.02, 69.60, 44.99, 39.36, 37.39, 32.47, 32.47, 29.45, 26.63, 25.38, 23.84, 16.52, 14.47.

(4-Fluoro-4-hydroxyethoxy-1,3,5,7-tetramethyl-8-(3-((2-(2-((6-chlorohexyl)oxy)ethoxy)ethyl)amino)-3-oxopropyl)-4-bora-3a,4a-diaza-s-indacene) ***17.*** To BODIPY **16** (3.1 mg, 0.006 mmol) in $CHCl_3$ (3 mL) was added TMSOTf from a 10% (v/v) stock solution in $CHCl_3$ (33 μL, 0.018 mmol) under stirring at 0 °C. After 2 min and 30 s activation, the reaction was quenched with ethylene glycol (∼100 equiv) and the reaction was allowed to stir for an additional 2 min. The mixture was then partitioned between a 1:1 solution of CH_2Cl_2:$NaHCO_3$ (sat). The organics were washed 3X with H_2O + 10% NaCl (sat), dried over Na_2SO_4, gravity filtered, and solvents removed in vacuo at room temperature. Purified on a silica gel column (1:1 Toluene:MeCN → 1:5 Toluene:MeCN + 1% MeOH) yielding an orange solid (2 mg, 0.0035 mmol, 60%). MS: $C_{28}H_{44}BClFN_3O_5$ Exact mass: 567.30; ES-$[M-H]^-$ Found: 566.22; ES+$[M + Na]^+$ Found: 590.33. ^{1}H NMR (400 MHz, benzene-d_6) δ 5.71 (s, 2H), 5.50 (brs, 1H−NH), 3.58 (brs, 1H−OH), 3.32−3.30 (m, 8H), 3.20−3.08 (m, 10H), 2.58 (s, 6H), 2.19 (d, J = 5.6 Hz 6H), 1.40−1.30 (m, 6H), 1.15−1.11 (m, 4H).

Fluorescent Turn-on Reaction Kinetics. 15 μL tetrazine-functionalized CMA-BODIPY **15** (20 μM) and 15 μL 4-*trans*-cyclooctenol (40 μM) stock solutions in PBS were combined in black, flat-bottom 384-well plates. Time-dependent fluorescence intensity increase was measured in TECAN Safire 2 multiwell plate reader (λ_{ex} = 490 nm, λ_{em} = 512 nm). All experiments were performed in triplicate.

Physical Characterization. *Stability Tests on Plate-Reader.* Stability tests were performed on a monochromator based TECAN Safire 2 multiwell plate reader. From 10 mM DMSO stock solutions, 10 μM dilutions of the title BODIPY derivatives and Fluorescein were prepared in 1X PBS (pH = 7.4) and cell imaging media [RPMI 1640 (+) 10% FBS and (−) phenol red]. 30 μL of replicates were transferred into black, flat-bottom 384-well plates. Fixed fluorescence intensity readings were acquired over 30 h under constant instrument settings. Excitation and emission wavelengths selected for monitoring were optimized for BODIPY analogues (λ_{ex} = 490 nm, λ_{em} = 512 nm). In between reads, plates were stored at room temperature and protected from light. Note that **9** and **12e** were analyzed in 1:1 1X PBS:DMF.

Stability Tests on Analytical LC-MS. From 10 mM DMSO stock solutions, 10 μM dilutions of the title BODIPY derivatives were prepared in 1X PBS (pH = 7.4). Replicates were stored, protected from light, either at room temperature or in a sterile incubator (37 °C, 5% CO_2). Over 24 h, neat aliquots were taken from these solutions at standardized time points and analyzed by analytical LC-MS. The multiwavelength fluorescence detector settings were optimized for monitoring BODIPY fluorescence (λ_{ex} = 490 nm, λ_{em} = 512 nm). Instrument gain and EUFS settings were maintained as constant values across runs during the time-course experiment.

Solubility Test. Solubility tests were performed on a monochromator based TECAN Safire 2 multiwell plate reader. Stock solutions for solubility tests were prepared by dissolving each compound (in quantities at least 2 mg and greater) in 1X PBS until fully saturated. Upon reaching saturation, solutions were centrifuged at 15 000 rpm for 10 min to ensure that no free particles were suspended in the supernatant. Aliquots from the saturated solution were removed and dissolved into DMSO (10-fold dilution). 30 μL aliquots of replicates were transferred into black, flat-bottom 384-well plates and fixed fluorescence intensity readings were acquired. The multiwavelength fluorescence detector settings were optimized for monitoring BODIPY fluorescence (λ_{ex} = 490 nm, λ_{em} = 512 nm). These values were referenced to concentration calibration curves (nM to mM) of each compound dissolved in DMSO acquired under identical instrument settings.

LogD Test. LogD tests were performed on a monochromator based TECAN Safire 2 multiwell plate reader. Prior to performing the experiment, a 1:1 mixture of 1-octanol (spectrophotometric grade) and 1X PBS were equilibrated for 24 h at room temperature. This equilibrated 1-octanol was used as the nonpolar cosolvent for logD measurements. To perform LogD, aliquots of the saturated 1X PBS stocks, described in the solubility test, were added to an equivalent volume of 1-octanol. The biphasic solutions were continuously and vigorously shaken for 1 h. Solutions were centrifuged for 2 min at 15 000 rpm to assist in layer separation and then aliquots (in triplicate) were removed from each layer and subsequently dissolved in DMSO (10-fold dilution). 30 μL aliquots of replicates were transferred into black, flat-bottom 384-well plates and fixed fluorescence intensity readings were acquired. The multiwavelength fluorescence detector settings were optimized for monitoring BODIPY fluorescence (λ_{ex} = 490 nm, λ_{em} = 512 nm). Each set of measurements (sat. 1X PBS

layer in DMSO and octanol layer in DMSO) per compound was obtained under identical instrument settings.

pH Fluorescence Test. pH-dependent fluorescence of CMA-BODIPY **12a** was measured using a monochromator based TECAN Safire 2 multiwell plate reader. Briefly, 10 mM stock solution of **12a** in DMSO were diluted into aqueous buffer (pH = 3, 5, 7.4, 10) at 100 μM, and transferred into black, flat-bottom 384-well plates (CORNING) and fluorescence intensity was acquired (λ_{ex} = 490 nm, λ_{em} = 512 nm) in duplicate.

Cell Culture. Cell lines were propagated following sterile technique using sterile incubators (37 °C, 5% CO_2). Cell culture media and supplements were sterile filtered prior to use and were obtained from Gibco (FBS, 1X Attachment Factor), Life Technologies (CO_2 Independent Medium, RPMI 1640, 1X PBS), and Invitrogen (RPMI 1640). Chemical reagents were obtained from Cell Signaling Technologies (Staurosporine), Promega (CellTiter-Glo Luminescent Cell Viability Assay), and Life Technologies (ER-Tracker Red). Culture and imaging plates were obtained from MatTek Corporation (No. 1.5 glass-bottom), COSTAR (Cat #9309), Lab-Tek (PA 19440), and MatriPlate (MGB096-1-2-LG-L).

MDA-MB-231 (pLVX H2B-mCherry) cells were a gift of Dr. Sarah Earley. MDA-MB-231 cells were cultured with RPMI 1640 1X [(+) phenol red, (+) 10% FBS, (+) 1% Pen-Strep]. PtK2 cells were cultured in 24 well No. 1.5 glass-bottom dishes with MEM [(+) 2% FBS + 1% Pen-Strep]. MCF-7 cells were obtained from ATCC (American Tissue Culture Collection) and cultured in 1X RPMI 1640 [(+) phenol red, (+) 10% FBS, (+) 1% Pen-Strep]. Prior to experiments, cells were confirmed mycoplasma free using a commercially available testing kit from Lonza (MycoAlert). Imaging data was analyzed with ImageJ software (http://rsbweb.nih.gov/ij).

Cell Viability Studies. 20 000 MCF-7 cells/well were seeded in 96-well cell culture plates. The next day, cells were incubated with varying concentrations of MayaFluors. Pentamethyl difluoro BODIPY and staurosporine were selected as positive controls, for 24 and 48 h incubation, respectively. Assay compounds were dispensed from 10 mM DMSO stock solutions using an HP D300 digital dispenser. Following incubation, cells were washed with 1X PBS and the cytotoxicity was evaluated using CellTiter-Glo Luminescent Cell Viability Assay Kit according to the manufacturer's protocol. Briefly, plates were taken out from incubator and equilibrated to room temperature for 30 min and a volume of CellTiter-Glo reagent was added to each well in a 1:1 ratio with the culture medium present in the assay wells. After 10 min incubation at room temperature to stabilize luminescent signal, the plates were read in a Luminescent Plate Reader (Envision, PerkinElmer 2103 Multi Reader). Control wells containing medium without cells were prepared to obtain background luminescence data. All assays were performed in duplicate.

Live Cell Imaging. *Imaging of Wash-Out Kinetics.* Live-cell imaging was performed on a Zeiss Axiovert 100 M inverted epifluorescence microscope with a 40X objective. Per region of interest, a bright field view was acquired as well as GFP and TexasRed fluorescence channels. Two days prior to imaging, MDA-MB-231 cells were seeded at 20 000 cells/well on a 96-well glass bottom microwell plate pretreated with 1X Attachment Factor. Imaging media was used for experiments, RPMI 1640 1X [(−) phenol red, (+) 10% FBS]. The day of imaging, each well was incubated for 30 min with 10 μM of the title compound suspended in cell imaging media (final DMSO content = 0.1%). Subsequently three washes were performed. Each wash consisted of removing spent media, adding fresh imaging media, and incubating the cells for 5 min. After each wash a thin layer of cell imaging media was added and wells were rapidly imaged. No imaging enhancing processing was performed for acquired data.

For confocal imaging of BODIPY and ER-tracker colocalization, images were acquired on a Leica TSC SP laser scanning spectral confocal microscope at 70X magnification (20X objective, 3.5 hardware zoom) as *z*-stacks with 1 μm step size. 40 000 MCF-7 cells/well were seeded in a 4 Chamber Glass Slide from Lab-Tek with 1 mL RPMI 1640 imaging medium supplemented with FBS. The next day, media was aspirated, cells were washed with 1X PBS, and 500 μL warm RPMI medium containing a final concentration of 10 μM difluoro-BODIPY and 1 μM ER-Tracker Red was added to the chambers and incubated for 1 h at 37 °C. Cells were washed once with PBS and covered with 500 μL PBS for immediate live-cell imaging. Maximum *z*-projection images were exported as tiffs and no further image enhancing processing was performed.

BODIPY Uptake Quantification. Images were acquired on a Nikon Eclipse Ti microscope system with a humidified chamber from InVivo Scientific to maintain a 37 °C environment. The microscope was equipped with a Mercury arc lamp, a PlanApo 60XA (NA = 1.4, Ph3 DM) oil objective, a Chroma FITC filter cube, and cooled charge-coupled device camera (CoolSNAP HQ, Roper Scientific). The microscopy system was controlled by Nikon Elements software. PtK2 cells were cultured in 24-well plates with CO_2 Independent Medium. For drug treatment and wash-out, each compound was added to live cells for a final concentration of 100 nM. The fluorescent images were immediately collected upon drug treatment. Then, wells were washed once with 1 mL fresh media and replaced with another 1 mL fresh media. After 5 min, the washout images were collected using 200 ms exposure time with 2-by-2 binning. Individual cells were selected by same size ROI (region of interest) for calculation of average intensity. A total of 29 cells (compound **9**), 23 cells (compound **12a**), 29 cells (compound **12b**), and 24 cells (compound **12c**) were used.

■ ASSOCIATED CONTENT

Supporting Information

NMR-spectra, comprehensive LC-MS stability data, absorption and emission spectra, pH-dependent fluorescence intensity of **12a**, cellular imaging data, turn-on kinetics of compound **15**. This material is available free of charge via the Internet at http://pubs.acs.org.

■ AUTHOR INFORMATION

Corresponding Author

*E-mail: rmazitschek@mgh.harvard.edu.

Notes

The authors declare no competing financial interest.

■ ACKNOWLEDGMENTS

Financial support from the NCI (P50CA086355, T32-CA079443) and Fundação para a Ciência e a Tecnologia (SFRH/BD/80162/2011) is gratefully acknowledged. We thank Drs. R. Weissleder and S. Haggarty for support and J. Carlson for helpful discussions.

REFERENCES

(1) Lavis, L. D., and Raines, R. T. (2008) Bright ideas for chemical biology. *ACS Chem. Biol. 3*, 142−155.

(2) Pepperkok, R., and Ellenberg, J. (2006) High-throughput fluorescence microscopy for systems biology. *Nat. Rev. Mol. Cell. Biol. 7*, 690−696.

(3) Tsien, R. Y. (2010) Fluorescence readouts of biochemistry in live cells and organisms, In *Molecular imaging: principles and practice* (Weissleder, R., Ross, B. D., Rehemtulla, A., and Gambhir, S., Eds.) pp 808−828, People's Medical Publishing House, Shelton, CT.

(4) Weissleder, R., and Pittet, M. J. (2008) Imaging in the era of molecular oncology. *Nature 452*, 580−589.

(5) Wennmalm, S., and Simon, S. M. (2007) Studying individual events in biology. *Annu. Rev. Biochem. 76*, 419−446.

(6) Johnson, T. W., Dress, K. R., and Edwards, M. (2009) Using the golden triangle to optimize clearance and oral absorption. *Bioorg. Med. Chem. Lett. 19*, 5560−5564.

(7) Shank, N. I., Pham, H. H., Waggoner, A. S., and Armitage, B. A. (2013) Twisted cyanines: a non-planar fluorogenic dye with superior photostability and its use in a protein-based fluoromodule. *J. Am. Chem. Soc. 135*, 242−251.

(8) Lukinavicius, G., Umezawa, K., Olivier, N., Honigmann, A., Yang, G., Plass, T., Mueller, V., Reymond, L., Correa, I. R. J., Luo, Z. G., Schultz, C., Lemke, E. A., Heppenstall, P., Eggeling, C., Manley, S., and Johnsson, K. (2013) A near-infrared fluorophore for live-cell super-resolution microscopy of cellular proteins. *Nat. Chem. 5*, 132−139.

(9) Ulrich, G., Ziessel, R., and Harriman, A. (2008) The chemistry of fluorescent bodipy dyes: versatility unsurpassed. *Angew. Chem., Int. Ed. Engl. 47*, 1184−1201.

(10) Beatty, K. E., Szychowski, J., Fisk, J. D., and Tirrell, D. A. (2011) A BODIPY-cyclooctyne for protein imaging in live cells. *ChemBioChem 12*, 2137−2139.

(11) Didier, P., Ulrich, G., Mely, Y., and Ziessel, R. (2009) Improved push-pull-push E-Bodipy fluorophores for two-photon cell-imaging. *Org. Biomol. Chem. 7*, 3639−3642.

(12) Hapuarachchige, S., Montaño, G., Ramesh, C., Rodriguez, D., Henson, L. H., Williams, C. C., Kadavakkollu, S., Johnson, D. L., Shuster, C. B., and Arterburn, J. B. (2011) Design and synthesis of a new class of membrane-permeable triazaborolopyridinium fluorescent probes. *J. Am. Chem. Soc. 133*, 6780−6790.

(13) Wang, S., Guo, J., Ono, T., and Kool, E. T. (2012) DNA polyfluorophores for real-time multicolor tracking of dynamic biological systems. *Angew. Chem., Int. Ed. Engl. 51*, 7176−7180.

(14) Zheng, Q., Xu, G., and Prasad, P. N. (2008) Conformationally restricted dipyrromethene boron difluoride (BODIPY) dyes: highly fluorescent, multicolored probes for cellular imaging. *Chemistry 14*, 5812−5819.

(15) Bura, T., and Ziessel, R. (2011) Water-soluble phosphonate-substituted BODIPY derivatives with tunable emission channels. *Org. Lett. 13*, 3072−3075.

(16) Niu, S. L., Ulrich, G., Ziessel, R., Kiss, A., Renard, P.-Y., and Romieu, A. (2009) Water-soluble BODIPY derivatives. *Org. Lett. 11*, 2049−2052.

(17) Zhu, S., Zhang, J., Vegesna, G., Luo, F.-T., Green, S. A., and Liu, H. (2011) Highly water-soluble neutral BODIPY dyes with controllable fluorescence quantum yields. *Org. Lett. 13*, 438−441.

(18) Gabe, Y., Ueno, T., Urano, Y., Kojima, H., and Nagano, T. (2006) Tunable design strategy for fluorescence probes based on 4-substituted BODIPY chromophore: improvement of highly sensitive fluorescence probe for nitric oxide. *Anal. Bioanal. Chem. 386*, 621−626.

(19) Jiang, X.-D., Zhang, J., Furuyama, T., and Zhao, W. (2012) Development of mono- and di-AcO substituted BODIPYs on the boron center. *Org. Lett. 14*, 248−251.

(20) Tahtaoui, C., Thomas, C., Rohmer, F., Klotz, P., Duportail, G., Mély, Y., Bonnet, D., and Hibert, M. (2007) Convenient method to access new 4,4-dialkoxy- and 4,4-diaryloxy-diaza- s-indacene dyes: synthesis and spectroscopic evaluation. *J. Org. Chem. 72*, 269−272.

(21) Hendricks, J. A., Keliher, E. J., Wan, D., Hilderbrand, S. A., Weissleder, R., and Mazitschek, R. (2012) Synthesis of [18F]BODIPY: bifunctional reporter for hybrid optical/positron emission tomography imaging. *Angew. Chem., Int. Ed. Engl. 51*, 4603−4606.

(22) Guo, B., Peng, X., Cui, A., Wu, Y., Tian, M., Zhang, L., Chen, X., and Gao, Y. (2007) Synthesis and spectral properties of new boron dipyrromethene dyes. *Dyes Pigm. 73*, 206−210.

(23) Wang, D., Fan, J., Gao, X., Wang, B., Sun, S., and Peng, X. (2009) Carboxyl BODIPY dyes from bicarboxylic anhydrides: one-pot preparation, spectral properties, photostability, and biolabeling. *J. Org. Chem. 74*, 7675−7683.

(24) Yang, J., Seckute, J., Cole, C. M., and Devaraj, N. K. (2012) Live-cell imaging of cyclopropene tags with fluorogenic tetrazine cycloadditions. *Angew. Chem., Int. Ed. Engl. 51*, 7476−7479.

(25) Bonnier, C., Piers, W. E., Parvez, M., and Sorensen, T. S. (2008) Borenium cations derived from BODIPY dyes. *Chem. Commun.*, 4593−4595.

(26) Hudnall, T. W., and Gabbai, F. P. (2008) A BODIPY boronium cation for the sensing of fluoride ions. *Chem. Commun.*, 4596−4597.

(27) Blackman, M. L., Royzen, M., and Fox, J. M. (2008) Tetrazine ligation: fast bioconjugation based on inverse-electron-demand Diels-Alder reactivity. *J. Am. Chem. Soc. 130*, 13518−13519.

(28) Devaraj, N. K., Weissleder, R., and Hilderbrand, S. A. (2008) Tetrazine-based cycloadditions: application to pretargeted live cell imaging. *Bioconjugate Chem. 19*, 2297−2299.

(29) Devaraj, N. K., Hilderbrand, S., Upadhyay, R., Mazitschek, R., and Weissleder, R. (2010) Bioorthogonal turn-on probes for imaging small molecules inside living cells. *Angew. Chem., Int. Ed. Engl. 49*, 2869−2872.

(30) Demchenko, A. P., Mély, Y., Duportail, G., and Klymchenko, A. S. (2009) Monitoring biophysical properties of lipid membranes by environment-sensitive fluorescent probes. *Biophys. J. 96*, 3461−3470.

(31) Loudet, A., and Burgess, K. (2007) BODIPY dyes and their derivatives: syntheses and spectroscopic properties. *Chem. Rev. 107*, 4891−4932.

(32) Los, G. V., Encell, L. P., McDougall, M. G., Hartzell, D. D., Karassina, N., Zimprich, C., Wood, M. G., Learish, R., Ohana, R. F., Urh, M., Simpson, D., Mendez, J., Zimmerman, K., Otto, P., Vidugiris, G., Zhu, J., Darzins, A., Klaubert, D. H., Bulleit, R. F., and Wood, K. V. (2008) HaloTag: a novel protein labeling technology for cell imaging and protein analysis. *ACS Chem. Biol. 3*, 373−382.

(33) Bergström, F., Mikhalyov, I., Hägglöf, P., Wortmann, R., Ny, T., and Johansson, L. B. Å. (2002) Dimers of dipyrromethene boron difluoride (BODIPY) with Light spectroscopic applications in chemistry and biology. *J. Am. Chem. Soc. 124*, 196−204.

(34) Campagnola, P. J., Wei, M. D., Lewis, A., and Loew, L. M. (1999) High-resolution nonlinear optical imaging of live cells by second harmonic generation. *Biophys. J. 77*, 3341−3349.

(35) Li, Z., Lin, T.-P., Liu, S., Huang, C.-W., Hudnall, T. W., Gabbai, F. P., and Conti, P. S. (2011) Rapid aqueous [18F]-labeling of a bodipy dye for positron emission tomography/fluorescence dual modality imaging. *Chem. Commun. 47*, 9324−9326.